HERA Dish Reflectometry

Nipanjana Patra, Zaki Ali, Carina Cheng, Dave DeBoer, Gilbert Hsyu, Tsz Kuk Leung, Aaron Parsons

1. Introduction

There are several different sources of instrumental chromaticity for radio telescope systems that can result in non-ideal performances and unwanted systematic effects in measured data. One such source is the mismatch between the impedance of free space and the feed and transmission line, which results in a partial coupling of the sky signal into the feed while the rest is reflected back into the space. For any reflector telescope, such as HERA, this signal illuminates the dish and part of it reflects back and forth several times in between the dish feed and the vertex of the dish. Such reflections generate multiple reduced strength copies of the incident sky signal at various delays, and this produces spurious correlations in the visibilities of interferometric data.

To first order, the design specification of HERA elements requires that any delayed signal, arriving at the feed after a multipath propagation, should be at the level of $-60dB$ at a delay of $60ns$ relative to the first incident signal at the feed (**?**). This specification was approximated based on the power level of the cosmological signal in relation to foreground signals, which is estimated to be six orders of magnitude fainter (**???????**). Additionally, the $14m$ HERA baselines set a foreground containing horizon-limit (the wedge) that, with some buffer, sets a delay specification of $60ns$ (**?????**).

We carry out reflectometry measurements at the HERA element prototype in Green Bank, WV (Figure **??**) in order to understand the nature of feed reflections in the dish and characterize its performance. As HERA progresses as an experiment, it is necessary to build optimized dishes that aim to minimize the challenges of chromaticity in our quest for the Epoch of Reionization.

2. Theory

Plane waves incident on a parabolic dish are focussed at the feed with focal height l. For a well-designed feed, one that closely matches the impedance of free space[1], most of the signal will enter the system while only a small percentage will be reflected back towards the dish for a secondary reflection into the feed (dashed blue arrows in Figure **??**). In the

[1]The impedance of free space is $Z_0 = \mu_0 c_0 = \frac{1}{\epsilon_0 c_0} \approx 377\Omega$.

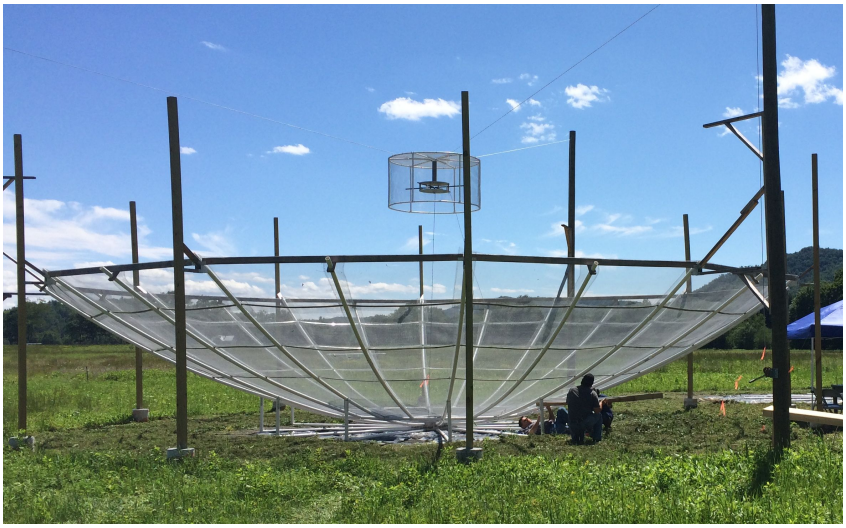

Fig. 1.— HERA dish and feed at the Green Bank NRAO site.

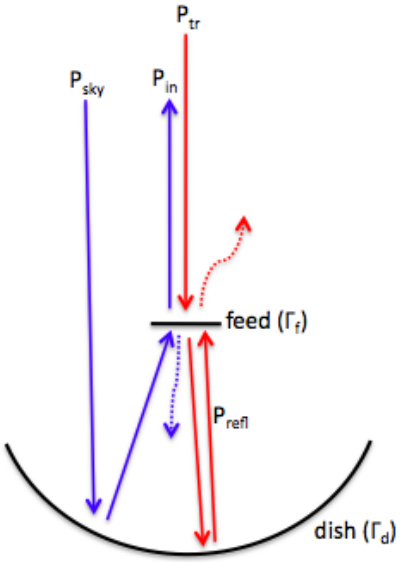

Fig. 2.— The blue solid lines represent an original sky signal entering the feed. A small percentage of it (dashed blue) is reflected off the dish, and it is these reflections that we are concerned about. In our measurements however, the reflections measured contain most of the original pulse signal (solid red), so it is crucial to adjust for this difference in our analysis.

following discussion, we consider a reflection off the feed and the subsequent reflection off the dish as one reflection.

Quantitatively, if the incident power from the sky signal is P_{sky}, the feed reflection coefficient is Γ_f, and the dish reflection coefficient is Γ_d, then the net power entering the feed after an n^{th} reflection off the feed and the dish is:

$$P_{in} = P_{sky}(1-\Gamma_f)[1+\Gamma_f\Gamma_d e^{i\phi} + (\Gamma_f\Gamma_d)^2 e^{i2\phi} + ... + (\Gamma_f\Gamma_d)^n e^{in\phi}] \quad (1)$$

where, $\phi = 2l(\frac{2\pi}{c})\nu$ is the propagation delay of a lightwave of frequency ν due to a reflection over a focal distance l. It is noted that upon the first incidence, the sky signal is focussed onto the feed from the entire dish and the dish reflection coefficient Γ_d is 1 for this first incidence. The subsequent back and forth reflection of the signal in between the feed and the dish, however, occurs from only the part of the dish which is shadowed by the feed. Therefore, in this case, $\Gamma_d < 1$.

Simplifying Equation **??**:

$$\begin{aligned}
\frac{P_{in}}{P_{sky}} &= (1-\Gamma_f)[1+\Gamma_f\Gamma_d e^{i\phi} + (\Gamma_f\Gamma_d)^2 e^{i2\phi} + ... + (\Gamma_f\Gamma_d)^n e^{in\phi}] \\
&= (1-\Gamma_f)\sum_{n=0}^{n}[\Gamma_f\Gamma_d e^{i\phi}]^n \\
&= (1-\Gamma_f) + (1-\Gamma_f)\sum_{n=1}^{n}[\Gamma_f\Gamma_d e^{i\phi}]^n \quad (2)
\end{aligned}$$

The ratio in Equation **??** quantifies the amount of power received with respect to the incident sky power. Realistically, the incident sky power is not easily quantifiable, but it is a quantity we need to know to accurately characterize reflections.

In our experimental set-up, instead of using sky signal, we employ our feed as a transmitter and transmit a pulse. If the initial pulse is a broadband signal, P_{tr}, sent to the feed via a $75ft$ cable by a vector network analyser (VNA), a delay domain measurement of the system is accomplished by taking the Fourier transform of the measured complex return loss of the feed. When the signal is incident on the feed, part of the incident power (Γ_f) is reflected back to the measuring device (dashed red arrows in Figure **??**) and $(1-\Gamma_f)$ is radiated by the feed (solid red arrows in Figure **??**) which illuminates the dish. While most of the incident signal is reflected back into space by the dish, the reflected signal from the dish vertex returns to the feed. This incident signal is now reflected back and forth in between the feed and the dish much like the sky signal reflection discussed previously. Hence, if P_r is the power incident back on the feed for the first time then the reflected power, P_{refl}, back into the VNA would be:

$$P_{refl} = P_r(1-\Gamma_f)[1+\Gamma_f\Gamma_d e^{i\phi} + (\Gamma_f\Gamma_d)^2 e^{i2\phi} + ... + (\Gamma_f\Gamma_d)^n e^{in\phi}] \quad (3)$$

Once again, note that we consider one reflection from the feed and its subsequent reflection from the dish as one reflection in total. Equation **??** is similar to Equation **??**, with different incident powers.

Recall that P_r is the initial power that is incident back on the feed, which is just the feed radiated power reflected off the dish:

$$P_r = \Gamma_d(1-\Gamma_f)e^{i\phi}P_{tr} \tag{4}$$

Also note that the first reflection of the signal sent by the VNA occurs at the feed end. Hence the total returned power P_{ret}, to the VNA would be:

$$\begin{aligned} P_{ret} &= \Gamma_f P_{tr} \\ &+ \Gamma_d(1-\Gamma_f)e^{i\phi}P_{tr}(1-\Gamma_f)[1+\Gamma_f\Gamma_d e^{i\phi}+....+(\Gamma_f\Gamma_d)^n e^{in\phi}] \end{aligned} \tag{5}$$

Simplifying:

$$\begin{aligned} \frac{P_{ret}}{P_{tr}} &= \Gamma_f + \Gamma_d(1-\Gamma_f)^2[e^{i\phi}+\Gamma_f\Gamma_d e^{i2\phi}+....+(\Gamma_f\Gamma_d)^n e^{in\phi}] \\ &= \Gamma_f + \frac{(1-\Gamma_f)^2}{\Gamma_f}\sum_{n=1}^{n}[\Gamma_f\Gamma_d e^{i\phi}]^n \end{aligned} \tag{6}$$

The ratio in Equation **??** is the returned power to the VNA with respect to the transmitted power sent by the VNA. It is identical to the sky observation case in Equation **??** but differs by two factors. The first factor corresponds to an additive amplitude difference arising from Γ_f, which physically accounts for the initial reflection at the feed. The second difference is a multiplicative term which informs us about the first reflection. Both of these terms need to be corrected for in order to relate our measurements to real observations.

The VNA measures the magnitude and phase of the quantity $\frac{P_{ret}}{P_{tr}}$ as a function of frequency as shown in Figure **??**. In our measurement set-up, the first reflection occurs at the feed Γ_f, so $(\frac{P_{ret}}{P_{tr}}-\Gamma_f)$ gives an estimate of the delay spectrum of the sky signal. In delay domain, the relative signal strength at zero delay represents the factor Γ_f while the signal strength at any other delay represents any delayed signal that enters the feed after being reflected from the feed surroundings.

3. Methodology

Our reflectometry measurements are made using a prototype HERA dish at NRAO in Green Bank, WV. The dish is a $14\,m$ diameter parabolic reflector structurally supported

with 3 telephone poles. The reflective material is made up of wire mesh that is attached to PVC pipes, forming the parabolic shape of the dish. With the current iteration of the HERA dish, the feed consists of a PAPER dipole encased in a cylindrical cage encompassing the backplane. The PAPER feed and the backplane (which is aimed at preventing feed-to-feed interaction between neighboring dishes) is raised and lowered by a three-pulley system. The focal height of the dish is $4.5m$ (~ 14.76ft).

Our measurements are made with a FieldFox in VNA mode. In this mode, a pulse is generated in the FieldFox and sent through a $75ft$ 50Ω cable that connects to the feed with a 4:1 passive balun. The magnitude and phase of the complex return loss is measured between 50 to $500MHz$ over 1024 frequency channels which gives a frequency resolution of 0.44MHz. The delay resolution of the measurements is $\Delta t = 2.22ns$. In addition, we note that the round trip of a reflection from the feed to the dish is $9m$, which corresponds to a delay of $30ns$.

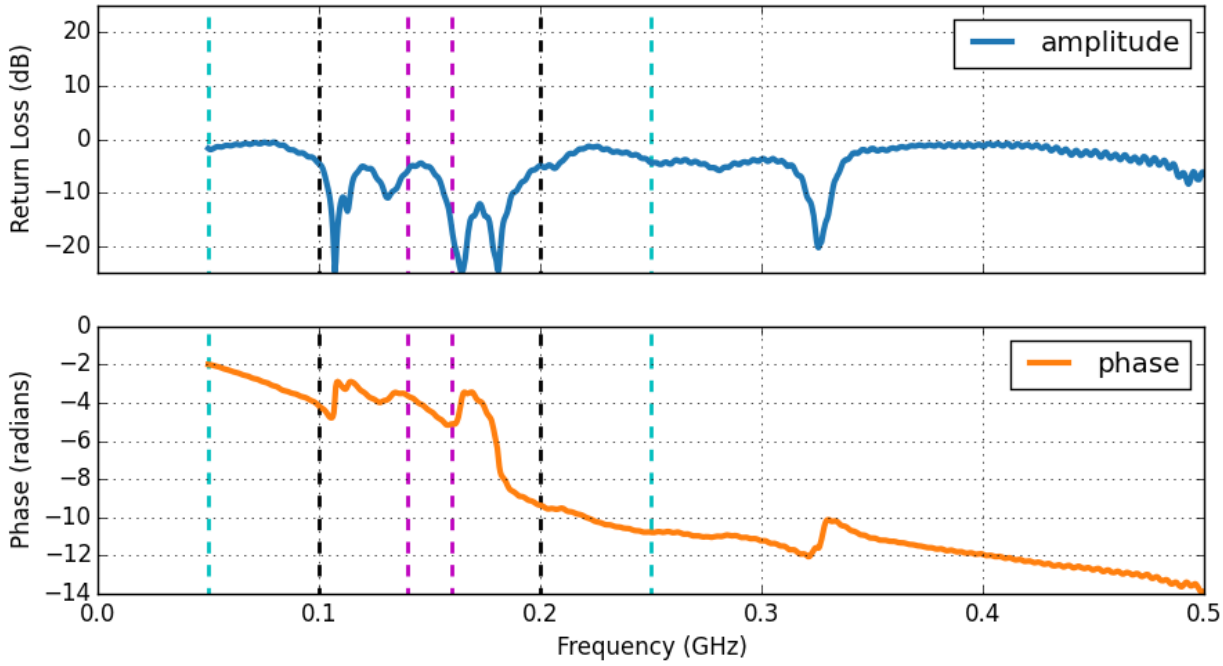

Fig. 3.— Amplitude and phase of the measured return loss. Colored dashed lines mark three different frequency bands: $140-160MHz$ (typical power spectrum bandwidth), $100-200MHz$ (PAPER bandwidth), and $50-250MHz$ (HERA bandwidth).

Frequency domain data, as shown in Figure **??**, can be Fourier-transformed to compute the return loss in the delay domain. Because the measured data is band-limited between 50 to $500MHz$, it is analogous to multiply the measured data by a square window function. Then in delay domain, the response would be convolved with a *sinc* function. This may result in excess power at high delays due to the sidelobes of the *sinc* function. Hence, appropriate windowing of the measured data set is necessary before taking the Fourier transform. We

have chosen a Hamming window for our analysis, and its effectiveness of this window function compared to others is illustrated in Figure **??**.

As mentioned in Section **??**, there is a mismatch in amplitude between the reflections that we measure (originating from the FieldFox pulse) and reflections produced by sky signal. The reflections that we measure (at high delays) must be lowered by a factor to represent weaker reflections that would occur after most of the sky signal is received by the feed. For our compensation, we multiply our entire delay spectrum by its DC component, which is the feed reflection coefficient Γ_f, and also divide by $(1 - \Gamma_f)$. In other words, these correction factors equate Equation **??** with Equation **??**. We note that this correction is only accurate at high delays where our reflections of interest occur. At low delays, our spectrum amplitude should be increased to represent the original sky signal, but we do not apply this correction because it is not relevant to our analysis.

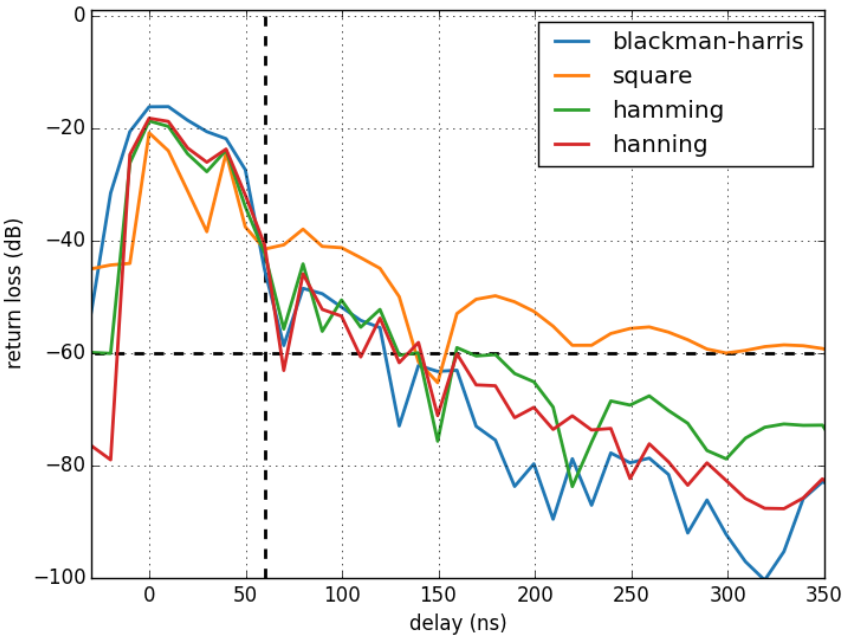

Fig. 4.— Delay plot produced for the PAPER bandwidth ($100MHz - 200MHz$) by taking the Fourier transform of the measured return loss using four different window functions: Blackman-Harris, square, Hamming, and Hanning.

4. Results

Figure **??** shows the return loss for a frequency bandwidth of 50 to $500MHz$. This measurement was taken with the feed suspended at $4.26m$, which was our closest measurement to the actual focal height. Because the return loss is the ratio of the power received to the

power transmitted, higher reflections can clearly be seen outside of the PAPER bandwidth. This is not surprising, since the feed is tuned specifically for PAPER. The return loss minima are locations where our feed is well-matched to free space.

In Figure **??**, the return loss we measure is plotted versus delay for three chosen bandwidths: the HERA bandwidth, the PAPER bandwidth, and a typical power spectra bandwidth when using a Hamming window function. Two additional measurements, using data taken in 2014 with the first prototype HERA dish near Berkeley, CA, are also plotted using two different bandwidths. One of the main differences between the Green Bank and Berkeley measurements is that the feed was not encompassed in a cage for the Berkeley data (only a backplane). Additionally, the $50 - 1000MHz$ data taken in Berkeley was Fourier-transformed internally by the measuring device, while the $100 - 200MHz$ data is analyzed post-measurement in the same way as the Green Bank data.

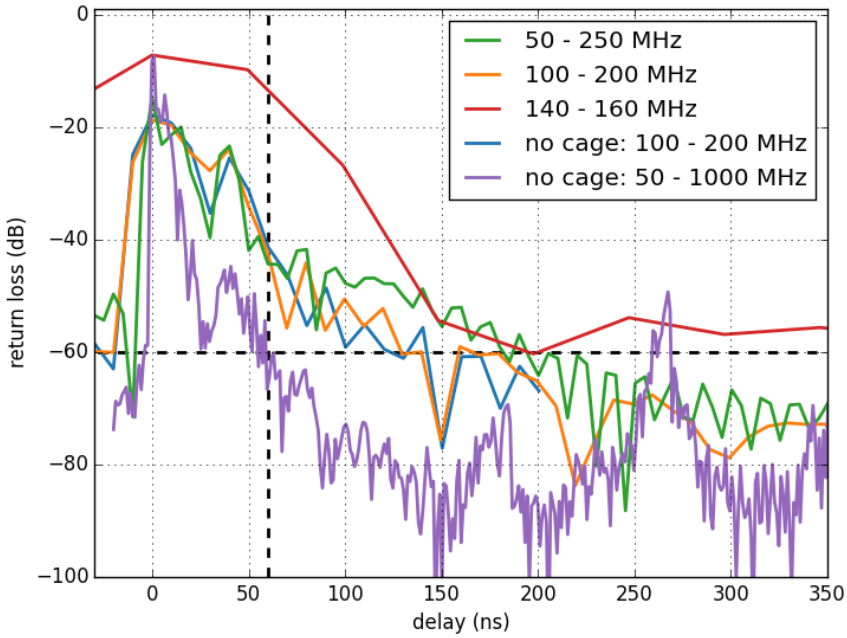

Fig. 5.— Delay plots produced using a Hamming window function for 5 different cases. Three of the cases correspond to measurements taken in Green Bank for three frequency bandwidths: $50MHz - 250MHz$ (HERA bandwidth), $100MHz - 200MHz$ (PAPER bandwidth), and $140MHz - 160MHz$ (typical power spectrum bandwidth). Two of the cases correspond to measurements taken in 2014 of the first prototype HERA dish in Berkeley (without a feed cage). Of these, we plot data for two frequency bandwidths: $100MHz - 200MHz$ (PAPER bandwidth), and $50MHz - 1000MHz$ (full bandwidth used by the VNA). For the PAPER bandwidth data, we follow the same Fourier-transform analysis as the others, while the full bandwidth data is produced directly by the VNA. The black dashed lines illustrate our "60 by 60" specification.

From the plot, we see that the delay response of a feed is dependent on the band chosen for the Fourier transform. As one might expect, in regions where the feed return loss is low, reflections are minimized. Thus, we cannot ignore that these measurements were performed using a PAPER-style feed tuned for efficient operation over a $100 - 200MHz$ bandwidth. Fourier transforms taken over wider bands become dominated by the feed performance in regions outside the operating band, making the resultant delay profiles less relevant for the power spectrum performance of the HERA instrument. Conversely, when performing Fourier transforms over much narrow bands (the windowed $20MHz$ bands typical of PAPER analysis), the width of the resulting delay profile becomes dominated by sidelobes of low delay emission interacting with the narrow bandwidth kernel. Although this may appear to be a relevant performance metric for PAPER-style power spectrum analysis, such an analysis typically pre-filters out low-delay emission using wide bandwidths precisely to avoid sidelobes from low-delay emission. Hence, the most relevant delay-spectrum performance profile is that taken using the $100 - 200MHz$ band.

In the $100 - 200MHz$ delay profile, we see a delay response of $-50dB$ at $60ns$, which slopes down to $-60dB$ at $\sim 120ns$. Because this does not achieve $-60dB$ attenuation at $60ns$, this indicates that the HERA system under test does not meet specification. However, we can learn additional information by evaluating different feed components.

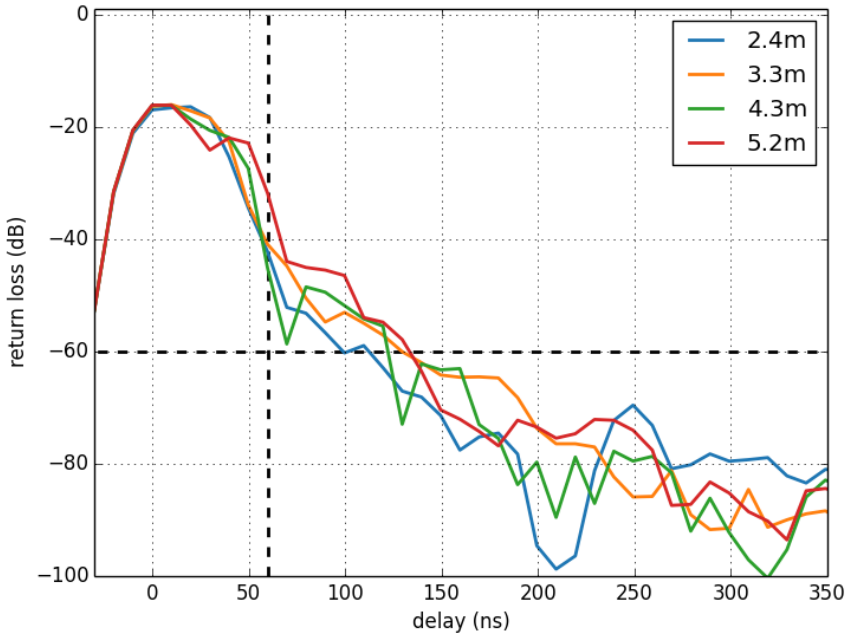

Fig. 6.— Delay plots produced using a Hamming window function for 4 different feed heights and the PAPER bandwidth ($100MHz - 200MHz$). The black dashed lines illustrate our "60 by 60" specification.

Figure **??** is again a delay plot of the return loss, but for four different feed suspension heights. We use the PAPER bandwidth and note that the measurements are near identical at low delays, implying that low delay reflections are caused primarily by reflections within the feed cage. However, at higher delays we notice discrepancies between the different heights.

In addition, Figure **??** presents measurements taken of the feed away from the dish. Echosorb is placed under the feed for some of the measurements, with the expectation that it will prevent any reflections off the ground. Measurements are also taken of the feed inside its metal cage in various configurations. It is shown that the feed performs best without the cage and with the absorber.

From these various measurements, we find that the feed itself is responsible for a significant portion of the structure up to $60ns$ and that the cylindrical cage may be contributing up to $20ns$ to the width of the delay profile. We note that this depends strongly on its coupling to structures around it. Structure beyond $60ns$ appears to scale with the height of the feed above the dish, making reflections off the dish the likely culprit.

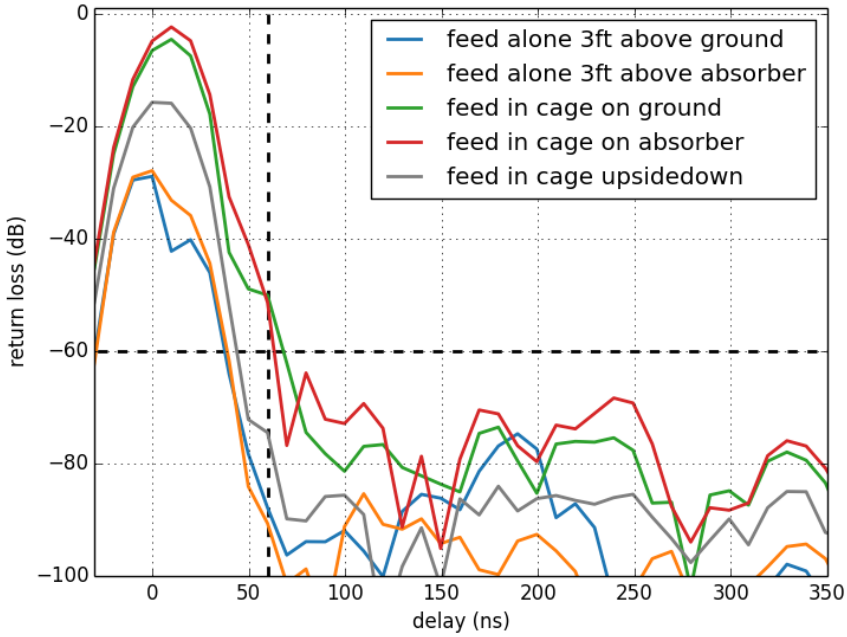

Fig. 7.— Delay plots produced using a Hamming window function for different lone feed configurations and the PAPER bandwidth ($100MHz - 200MHz$). The black dashed lines illustrate our "60 by 60" specification.

5. Conclusion

The delay-domain performance of the HERA dish is central to HERA's function as a power spectrum instrument. As we have seen, reflectometry measurements can help characterize HERA's performance in this domain, and as Equation **??** shows, these measurements must be adjusted for a difference in transmission/reflection at the first feed encounter in order to be interpreted as the delay response of a feed relative to an incident plane wave from the sky. We also see that the choice of windowing function is critical for accurately measuring the antenna delay response at higher delays, where sidelobes from much higher amplitude responses at small delays can easily dominate. We find Hamming, Hanning, and Blackman-Harris windows to be generally adequate while square windowing functions are not. Given the critical nature of the windowing function, we recommend that all reflectometry measurements be performed in the frequency domain, so that the data analyst can manually implement the Fourier transform with the appropriate window.

Taken all together, we summarize that the first version of the HERA dish, with a PAPER-style feed and cylindrical cage, is close to meeting specification, but will require additional work to fall below $-60dB$ at $60ns$. Given that the width of the delay response is a convolution of the feed response and the dish reflections, it is not possible to perfectly decouple the response of the feed from that of the dish. It may be possible to achieve enough of a reduction to meet specification by modifying the feed. Given that previous measurements using a PAPER feed with a simple backplane exhibit structure above $-60dB$ at $60ns$, we deduce that these advances will most likely require improving the feed return loss. We also recommend re-investigating the scattering cone for reducing standing waves between the feed and dish. Finally, given the proximity of our measurements to the rough specification that was adopted for HERA of $-60dB$ attenuation at $60ns$, we recommend reinvestigating this specification to determine more accurately the impact of the element's current delay performance on HERA science. We suspect that, at the level of $-50dB$ at $60ns$ and $-60dB$ at $120ns$, this performance may indeed be adequate for the delay-domain power spectrum analysis for which HERA has been optimized.

REFERENCES

Ali, S. S., Bharadwaj, S., & Chengalur, J. N. 2008, MNRAS, 385, 2166

Bernardi, G., de Bruyn, A. G., Brentjens, M. A., et al. 2009, A&A, 500, 965

Bernardi, G., de Bruyn, A. G., Harker, G., et al. 2010, A&A, 522, A67+

de Oliveira-Costa, A., Tegmark, M., Gaensler, B. M., et al. 2008, MNRAS, 388, 247

Ghosh, A., Bharadwaj, S., Ali, S. S., & Chengalur, J. N. 2011, MNRAS, 418, 2584

Jelić, V., Zaroubi, S., Labropoulos, P., et al. 2008, MNRAS, 389, 1319

Liu, A., Parsons, A. R., & Trott, C. M. 2014a, Phys. Rev. D, 90, 023018

—. 2014b, Phys. Rev. D, 90, 023019

Parsons, A. R., & DeBoer, D. D. 2015

Parsons, A. R., Pober, J. C., Aguirre, J. E., et al. 2012, ApJ, 756, 165

Santos, M. G., Cooray, A., & Knox, L. 2005, ApJ, 625, 575

Thyagarajan, N., Udaya Shankar, N., Subrahmanyan, R., et al. 2013, ApJ, 776, 6

Vedantham, H., Udaya Shankar, N., & Subrahmanyan, R. 2012, ApJ, 745, 176